scientific reports

Check for updates

OPEN

Fetal microchimeric cells influence maternal lung health following term and preterm births

Ananth Kumar Kammala[1]✉, Ryan C. V. Lintao[1,2], Richa Hoy[3], Jessica Selim[1,3], Jonathan Luisi[4,5], Jerome L. Yaklic[6], Bill T. Ameredes[4,5] & Ramkumar Menon[1]✉

Fetal microchimerism, the presence of fetal cells in maternal tissues, has garnered interest for its potential role in maternal physiology. In this study, we aimed to explore the impact of fetal microchimeric cells on maternal lung health following term and preterm delivery, particularly in the context of infection-induced preterm birth and subsequent allergic challenges. We characterized the immune cells in maternal lungs using a transgenic mouse model (mT+Ve, Td Tomato) and high dimensional mass cytometry (CyTOF) techniques. We evaluated their influence on lung function and inflammation. Our findings revealed distinct differences in the immune cell composition of maternal lungs between term and preterm deliveries. Mice delivered preterm significantly increased in fetal-specific cells, such as activated macrophages and Tbet+Ve memory B-cells, compared to term-delivered mice. Conversely, term deliveries showed elevated levels of CD4 cells. Furthermore, preterm-delivered dams demonstrated heightened airway hyperresponsiveness, pro-inflammatory cytokine expression, cellular infiltration, and lung mucous production compared to term-delivered dams. Co-culture experiments demonstrated that microchimeric cells from preterm births stimulated the production of inflammatory cytokines IL-6 and TNF-α in lung epithelial cells. These findings shed light on the complex immune dynamics postpartum and their role in lung complications after preterm birth. Understanding these mechanisms could provide insights for targeted interventions to improve maternal lung health in at-risk populations.

Keywords Preterm birth, Maternal lung, Fetal microchimerism

The intricate relationship between a mother and a developing fetus during pregnancy involves the exchange of cells, cellular components, and extracellular vesicles[1–6]. Fetal microchimerism, characterized by fetal cells in the maternal body that can persist for decades after pregnancy, has emerged as a captivating and enigmatic aspect of this complex existence[7–9]. The nature of these fetal microchimeric cells (FMCs) and their functional relevance within the maternal body remain a subject of ongoing studies and may hold potential answers regarding the modification of organ system responses in the mother over a lifetime.

FMCs exhibit remarkable pluripotency and immune competence, encompassing a diverse range of differentiated cell types[8,10]. They have been discovered in various maternal tissues, raising questions about their potential benefits and risks. FMCs have been associated with tissue repair, regeneration, and immunomodulation, suggesting a potential role in maternal health[5,11–16]. Conversely, there have been links between FMCs and neoplastic progression, as well as autoimmune diseases, underscoring the complexity of fetal microchimerism[17–19]. This duality emphasizes the need for comprehensive research to elucidate its mechanisms and consequences.

Recent data has indicated the presence of FMCs in maternal lungs persist after parturition which suggests a potential physiological or pathological role for these cells in lung tissue[8,20,21]. It is hypothesized that fetal cells enter the maternal lung tissue through circulation, but, their specific role in the lungs or other organ systems

[1]Division of Basic Science and Translational Research, Department of Obstetrics & Gynecology, The University of Texas Medical Branch at Galveston, 301 University Blvd., Galveston, TX 77555-1062, USA. [2]Department of Biochemistry and Molecular Biology, College of Medicine, University of the Philippines Manila, Manila, Philippines. [3]John Sealy School of Medicine, The University of Texas Medical Branch at Galveston, Galveston, TX, USA. [4]Department of Internal Medicine, The University of Texas Medical Branch at Galveston, Galveston, TX, USA. [5]Department of Pharmacology and Toxicology, The University of Texas Medical Branch at Galveston, Galveston, TX, USA. [6]Department of Obstetrics & Gynecology, The University of Texas Medical Branch at Galveston, Galveston, TX, USA. ✉email: ankammal@utmb.edu; ra2menon@utmb.edu

remains elusive and an ongoing area of investigation. Based on previous studies, it is reasonable to speculate that FMCs entering the maternal lungs at different gestational ages and during term pregnancies may exhibit distinct characteristics and have specific functional contributions. The current study was primarily focused on demonstrating the association between FMCs and lung function, with a long-term focus on unraveling the precise role of FMCs within the maternal lung tissue.

The FMCs migrating to maternal tissues includes immune and non-immune cells, as well as cells with stem cell properties[22]. In a normal pregnancy, FMCs may play a role in regenerating the maternal organs and restoring normalcy after the physiological and structural changes that occur during gestation[23]. We hypothesized that the number, type, and functional properties of FMCs at their destination sites will differ when comparing FMCs originating from pregnancies associated with specific risk factors, such as preterm birth, to those from uncomplicated term pregnancies.

To test this hypothesis, we employed a transgenic mouse model. This model features a membrane-targeted, two-color fluorescent Cre-reporter allele (mT/mG construct), where mT (red fluorescence) is exclusively expressed in fetal cells[24]. By mating female wild-type mice with homozygous males carrying the mT construct, we generated offspring with mT expression (mT+) specifically in fetal cells, but not in maternal cells. Subsequently, we investigated the migration patterns of FMCs during term and preterm pregnancies, particularly in ascending infections, and assessed their characteristics and functional impact both in vivo within the lung tissues and in vitro in alveolar epithelial cells.

This study not only aims to shed light on the intricate and intriguing phenomenon of FMCs, but also to elucidate its potential clinical implications, particularly in the context of maternal lung health. By discerning the distinct roles and behaviors of FMCs from different gestational backgrounds, we strive to contribute to a deeper understanding of this fascinating aspect of maternal–fetal biology and explore its relevance to both normal and high-risk pregnancies.

Materials and methods

Animal care

All animal procedures were approved by the Institutional Animal Care and Use Committee (IACUC) at the University of Texas Medical Branch at Galveston. For ascending infection and immune cell-trafficking studies, a cyclic recombinase (Cre)-reporter mouse model previously described by Sheller-Miller et al.[25] was used. Wild-type C57BL/6J (Strain #000664) and transgenic B6.129(Cg)-*Gt(ROSA)26Sor*$^{tm4(ACTB-tdTomato,-EGFP)Luo/J}$ (Strain #007676) mice were obtained from The Jackson Laboratory (Bar Harbor, ME). This transgenic mouse, referred to as mT/mG, has a two-color fluorescent Cre-reporter allele targeting the plasma membrane of all cells and tissues[26]. In the absence of cyclic recombinase, tandem dimer Tomato (tdTomato) red fluorescent protein (RFP) is expressed in the plasma membrane of all cells and tissues. As these mice are fertile, all cells and tissues of the progeny express tdTomato when homozygous males are mated with wild-type C57BL/6 females, while the cells and tissues of maternal origin do not express this RFP. This study was conducted and reported in accordance with ARRIVE guidelines (https://arriveguidelines.org)[27]. The mice were housed in a temperature- and humid ity-controlled facility with 12:12-h light and dark cycles. Regular chow and drinking solutions were provided ad libitum. Eight- to twelve-week-old wild-type females were mated with mT/mG homozygous males. Females observed with vaginal plugs in the morning, indicating gestational day 0.5 (E0.5), were housed separately from the males. A gain of at least 1.75 g by E10.5 confirmed pregnancy. A cohort of female mice not mated with males was maintained as the non-pregnant control (n = 5).

Polymerase chain reaction analysis

To determine the origin of fetal-specific cells in maternal tissues, polymerase chain reaction (PCR) was performed for the SRY gene on the Y chromosome. RNA was extracted from isolated maternal tissues (lungs, placenta, uterus, and kidney) using TRIzol® reagent (Invitrogen, Life Technologies), followed by chloroform (Fisher Scientific) and isopropanol (Acros Organics) treatments to purify total RNA. Total RNA was reverse-transcribed into complementary DNA (cDNA) with a high-capacity RNA-to-cDNA kit (Applied bio-systems). cDNA was then amplified by PCR using the RED Taq®Ready MixTM PCR reaction mix (Sigma) with the specific primers (for SRY gene, forward: 5′-TGGCGATTAAGTCAAATTCGC-3′ and reverse: 5′-CCCTAGTACCCTG ACAATGTATT-3′; for GAPDH gene, forward: 5′-ACCACAGTCCATGCCATCAC-3′ and reverse:5′-TCCACC ACCCTGTTGCTGTA-3′), according to the manufacturer's instructions. The PCR amplification was conducted using an iCycler thermal cycler (Bio-Rad) under the following conditions: 5 min at 94 °C denaturation, followed by 40 cycles at 94 °C for 30 s, 58 °C for 45 s, and 72 °C for 45 s. The PCR products (137 bp for SRY, 452 bp for GAPDH) were then analyzed with 1.5% agarose gel electrophoresis. The lung tissues collected from a male mT+ served as a positive control.

Model of ascending infection-induced preterm birth (PTB)

The detailed protocol for inducing ascending infection by *E. coli* has been previously described[28,29]. In brief, varying doses of *E. coli* (10^4 CFU) in 40-µL nutrient broth (Difco, Cat. # 234000, BD Biosciences, Franklin Lakes, NJ, USA) were vaginally administered to pregnant C57BL/6J mice using a blunt 200-µL pipette tip on gestational day E15. The timing of delivery, defined as the delivery of the first pup, was monitored using live cameras (Shenzen Wansview Technology, Shenzen, China). Delivery on or before E18.5 was considered preterm. A subset of pregnant C57BL/6 mice (n = 6) was euthanized at E16 via carbon dioxide inhalation, following IACUC and the American Veterinary Medical Association guidelines, to collect the maternal lung tissues.

Immunofluorescent imaging for mT signal in the maternal lung tissues

Tissue samples were collected from pregnant mice on E16 and were fixed in 4% paraformaldehyde and stored overnight at 4 °C before being washed twice with 1× PBS and transferred to a 15% sucrose solution overnight at 4 °C. The samples were then transferred to 30% sucrose and were stored at 4 °C until they were embedded in the optimal cutting temperature compound and cut into 5-mm sections. The sections were incubated at room temperature for 30 min and were then washed twice in water to remove the optimal cutting temperature compound. The sections were incubated with DAPI for nuclear staining for 2 min at room temperature and were then washed twice in water. To reduce the autofluorescence, tissues were incubated for 10 s with TrueVIEW Autofluorescence Quenching Kit (Vector Laboratories, Burlingame, CA), then washed twice with 1× Tris-buffered saline + Tween 20 (TBS-T). The slides were air-dried at room temperature for 10 min and then mounted using a mounting medium.

Immune cell isolation from the maternal lung tissue

The collected postpartum-term and preterm maternal lung tissues were cleaned using fine forceps to remove excess fat and were washed in cold 1× phosphate-buffered saline (PBS) (pH 7.4). Using fine scissors, the lung tissues were cut into small pieces and were digested with ([30–33]) Accutase cell-detachment solution (Corning, Corning, NY, USA) for 35 min at 37 °C with gentle rocking. While on ice, the tissue samples were strained through a 70-µm cell strainer and were washed twice with 10.0 mL of 1× PBS. After centrifugation at 1250 g for 10 min at 4 °C, the resulting cell pellets were resuspended in 2.0 mL of 1× red blood cell lysis buffer (BioLegend, San Diego, CA, USA) and incubated for 10 min at room temperature. Following lysis, the cell suspension was centrifuged at 1250 g for 10 min at room temperature. The supernatant was removed, and the cell pellet was resuspended in 1.0 mL of serum-free DMEM/Nutrient Mixture F-12 medium (DMEM/F12; Mediatech, Manassas, VA, USA). The cell suspension was overlaid gently on 500 µL of neat fetal bovine serum (FBS) (Sigma-Aldrich., Burlington, MA, USA) and the resulting mixture was centrifuged at 1100 g without brake for 10 min at room temperature. After carefully discarding the supernatant, the cell pellet was resuspended in 1.0 mL of DMEM/F-12 supplemented with 10% FBS.

High-dimensional single-cell profiling of fetal membrane tissues by mass cytometry

The CyTOF panel was designed based on the high-throughput screening results and also included proteins known to regulate myeloid cell functions (such as MerTK and Axl), transcription factors, and signaling molecules known to be relevant to inflammation during pregnancy (NF-κB and MAPK pathway). A summary of antibodies used for each panel is shown in Table 1. The antibodies were sourced from the MD Anderson Cancer Research Center Flow core facilities (MDACC, Texas, Houston), or were custom conjugated using the Maxpar antibody conjugation kit (Fluidigm, Markham, ON, Canada), following the manufacturer's protocol. After being labeled with their corresponding metal conjugate, the percentage yield was determined by measuring their absorbance at 280 nm using a Nanodrop 2000 spectrophotometer (Thermo Scientific, Wilmington, DE). The antibodies were diluted to 0.3 mg/mL using the Candor PBS antibody stabilization solution (Candor Bioscience GmbH, Wangen, Germany) and then stored at 4 °C.

Antibody staining

Single-cell suspension samples were resuspended in Maxpar staining buffer for 10 min at room temperature on a shaker to block Fc receptors. The cells were mixed with a cocktail of metal-conjugated surface marker antibodies (Table 1), yielding 500-µL of final reaction volumes, and then were stained at room temperature for 30 min on a shaker. Following staining, the cells were washed twice with Maxpar staining buffer. Next, the cells were permeabilized with Max Perm Buffer for 10 min at 4 °C. The cells were then washed twice in Maxpar staining buffer to remove the remaining Max Perm, and then stained with intracellular antibodies in 500 µL for 30 min at room temperature on a shaker. The samples were then washed twice in Maxpar staining buffer. The cells were incubated overnight at 4 °C with 1 mL of 1:4000 191/193Ir DNA intercalator (Standard BioTools, Inc., Markham, ON) diluted in Maxpar fix/perm. The following day, the cells were washed once with Maxpar staining buffer and then two times with double-deionized water (ddH20).

S.NO.	Cluster profiling	Cluster characterization	References
1	Ly6A-E, CD86, CD14, FOXp3, IFN-γ, CD11C, CD45	Activated Macrophages	[52–54]
2	CD8a, CD45	CD8	[55–58]
3	CD86, cd14, FoxP3, CD117, GATA-3	Mast cells	[58,59]
4	Cd86, FoxP3, IFN-γ, CD11c, TCR, GATA-3, T-bet	T-bet + Ve Memory B-cells	[60–63]
5	NK1.1	NK cells	[64,65]
6	CD4	CD4 cells	[65]
7	Ly6A-E and Siglec-F	Neutrophils	[64–67]
8	MHC-II and CD-19	B-cells	[68,69]

Table 1. mT+ -expressing cell clusters in the maternal lungs.

Mass cytometry

Prior to analysis, the stained and intercalated cell pellet was resuspended in ddH2O containing polystyrene normalization beads containing lanthanum-139, praseodymium-141, terbium-159, thulium-169, and lutetium-175, as described previously [59]. Stained cells were analyzed on a CyTOF 2 (Standard BioTools Inc, Markham, ON) outfitted with a Super Sampler sample introduction system (Victorian Airship & Scientific Apparatus, Alamo, CA) at an event rate of 200–300 cells per second. All mass cytometry files were normalized using the mass cytometry data normalization algorithm freely available for download from https://github.com/nolanlab/bead-normalization.

Data analysis

CyTOF data sets were first manually gated using the Standard BioTools/Fluidigm clean-up procedure with Gaussian discrimination (Markham, ON) in FlowJo V10 (FlowJo LLC). Each sample was given a unique Sample ID and then all samples were concatenated into a single .fcs file. This concatenated file was further analyzed by T-Distributed Stochastic Neighbor Embedding (t-SNE) in FlowJo V10, using equal numbers of cells from preterm delivered, term delivered mouse lungs tissue, all surface markers, and the following settings: iterations, 3000; perplexity, 50; and eta (learning rate), 4105. Heat maps of marker expression were generated using the Color Map Axis function. To explore the phenotypic diversity of immune cell populations in the different groups of mouse FM tissues, we applied a K-nearest-neighbor density-based clustering algorithm called Phenograph. This algorithm allows for the unsupervised clustering analysis of data from single cells. The output is organized using a cluster explorer tool to visualize the phenotypic continuum of cell populations. This tool creates an interactive cluster profile graph and a heat map and displays the cluster populations on a tSNE plot.

HDME-induced allergic lung inflammation models

For this study, House dust mice extract (HDME) induced murine models of allergic lung inflammation were employed (Fig. 3A) following established protocols[31,32]. Briefly, mice were challenged with seven doses of HDME (50 ug) on every alternate day. To investigate potential pregnancy-associated effects, mice of the same age group, including both term delivery and preterm delivery mice, were categorized into four distinct groups and were subjected to specific treatments. **Group 1** (n = 5) consisted of healthy, pregnant mice treated with PBS, **Group 2** (n = 5) involved exposing healthy, pregnant mice to an HDME challenge, **Group 3** (n = 5) comprised preterm, pregnant mice treated with PBS, and **Group 4** (n = 5) entailed preterm mice challenged with HDME.

Following the final HDME challenge, mice were anesthetized using a mixture of 100 mg/kg of ketamine, 10 mg/kg of xylazine, and 3 mg/kg of acepromazine. A tracheostomy was performed, and the forced oscillation technique was employed to measure airway mechanics, utilizing a small animal ventilator (flexiVent, SCIREQ Scientific Respiratory Equipment, Montreal, QC, Canada). Central airway resistance (Rn) was assessed upon stimulation with methacholine (Mch). Afterward, blood, bronchoalveolar lavage fluid (BALF), and lung tissues were collected for subsequent endpoint analyses.

Quantitative real-time PCR

RNA from mouse lungs was reverse transcribed into cDNA using the high-capacity cDNA Reverse Transcription Kit or the TaqMan Advanced miRNA cDNA Synthesis Kit (Applied Biosystems, Foster City, CA). Real-time quantitative PCR was performed using Quant Studio 3 (Applied Biosystems) with validated TaqMan primers and the Fast Advanced Master Mix. Relative gene expression data (fold change) between samples were accomplished using the 2-ΔΔCt method. GAPDH (for gene expression) was used as the internal control.

Evaluation of lung inflammation and goblet cell hyperplasia

Lung sections were prepared and were subjected to staining with H&E to examine lung inflammation and periodic acid-Schiff (PAS) to assess goblet cell hyperplasia[31,32]. The methodology involved the infusion of the lungs with 10% buffered formalin through the trachea. After excision, the lungs were immersed in fresh 10% formalin and left overnight. Subsequently, the samples were embedded in paraffin, sliced into sections with a thickness of 5 mm, and stained with either H&E or PAS. To capture digital images of the sections, a Nikon Eclipse 50i microscope equipped with an Infinity-3 Digital Color Camera from Teledyne Lumenera and Infinity Analyze 6.5.4 software were utilized. The sections were anonymized and assessed in a blinded manner for scoring.

Inflammation scoring

For inflammation scoring, multiple images encompassing the entire lung section were acquired at a magnification of 4× to determine the total count of bronchioles demonstrating the presence of infiltrated inflammatory leukocytes. Each bronchiole was assigned a score ranging from 0 to 4. Scores of 0–1 denoted no inflammation or the sporadic occurrence of inflammatory cells, while scores of 2–4 indicated bronchioles surrounded by a thin layer (two to four cells) of inflammatory cells. Scores exceeding 4 indicated bronchioles enclosed by a thick layer (more than five cells) of inflammatory cells. The number of bronchioles falling into each category (0–1, 2–4, or > 4) was then divided by the total number of inflamed bronchioles, resulting in the percentage of bronchioles within each inflammation category. To calculate the percentage severity of inflammation, the number of inflamed bronchioles scoring 4 or higher was divided by the total number of inflamed bronchioles. Goblet cell hyperplasia was evaluated on lung sections stained with PAS[32]. Each lung sample was divided into nine imaginary sections, and digital images were captured at a magnification of 10× to ensure consistent observation of identical regions across all samples and experiments. The intensity of PAS staining was analyzed using ImageJ software to determine the count and percentage area of PAS-positive cells in each section.

In vitro functional assay of fetal microchimeric cells

Cell isolation and culture

FMCs were sorted from mice of both term and preterm deliveries by FACS, utilizing a transgenic model in which fetal cells expressed the mT+ fluorescent marker. This enabled the efficient identification and isolation of fetal-specific cells (Fig. 4A). The isolated FMCs were cultured and maintained under appropriate conditions.

Co-culture experiment

Human small airway epithelial cells (HSAECs) were cultured according to the supplier's instructions (Lonza, Basel, Switzerland). FMCs (10,000 cells) obtained from the term and preterm deliveries from the previously isolated cell population were co-cultured with HSAECs in 24-well plates, as shown in Fig. 4A. This co-culture system aimed to mimic the interaction between FMCs and lung epithelial cells in a controlled environment.

Challenge with HDME

To assess the response of the co-cultured cells, HSAECs were challenged with HDME at a concentration of 5 µg/mL. HDME was chosen to induce a relevant inflammatory challenge in the HSAECs. This challenge was performed both with and without the presence of FMCs to investigate the potential modulatory effects of FMCs on the cellular response to HDME (Fig. 4B).

Supernatant collection and cytokine analysis

Following the incubation period of 24 h, the supernatant from the co-culture experiments was collected. The supernatant contained secreted factors that could reflect cellular responses. Cytokine analysis was performed on the collected supernatant samples to evaluate the inflammatory status of the lung epithelial cells. This analysis aimed to uncover any variations in cytokine profiles that might result from the interaction between FMCs and HSAECs (Fig. 4B).

The entire experimental procedure aimed to simulate the interaction between FMCs and HSAECs under different conditions to assess the potential impact of FMCs on HSAEC inflammation. The co-culture approach provided insights into the intricate interplay between FMCs and lung health, while the cytokine analysis allowed for the quantification of inflammatory responses, contributing to a comprehensive understanding of this cellular interaction.

Statistical analysis

Statistical analysis was performed using the GraphPad Prism 10.0 software (GraphPad, San Diego, CA). Statistical parameters associated with the figures are reported in the figure legends. All data are reported as the mean ± SEM. The statistical significance in differences between experimental groups and controls was assessed as follows: non-parametric and unpaired t-test for *E. coli* dose-dependent PTB study and Fisher's exact test for the rates of PTB. Significance was considered at $p < 0.05$.

Results

Characterization of fetal-specific immune cells in the maternal lungs

A previously described animal model of pregnancy, in which only fetal cells expressed TdTomato (mT+), allowed us to characterize fetal cells on the maternal side to study their impact on maternal physiology and/or pathology[25]. Wild-type C57B6/J females were mated with mT+ homozygous males (Fig. 1A) to show that fetal cells express TdTomato in the maternal tissues. At E16, the lungs, placenta, uterus, and kidney showed expression of the SRY gene, supporting the presence of microchimeric cells from the male progeny. Female wild-type lung cells and male mT+ homozygous lung cells were considered as the negative and positive controls, as shown in Fig. 1B. The propagation of fetal-specific cells in the maternal lungs during preterm pregnancy was determined by observing maternal lung tissue sections from non-pregnant, term delivery, and preterm delivery mice under the Keyence fluorescence microscope, as shown in Fig. 1C.

Profiling fetal-specific immune cells in maternal lungs

CYTOF analysis reveals distinct populations under varying pregnancy conditions

Among the 31 clusters generated using Phenograph (k = 183), we identified eight clusters expressing mT+, constituting approximately 20% of the maternal lung cell population. Unsupervised clustering analysis generated detailed t-SNE maps and cluster explorer-generated heat maps, providing insights into the parameter-intensity distribution within clusters across preterm delivery (PTD) and term delivery (TD) groups at the 24-h time point (Fig. 2A and B). The details of cluster characterization are shown in Table 1. Cluster 1 mT+ cells were of an activated macrophage phenotype, marked by the presence of Ly6A-E, CD86, FoxP3, IFN-γ, CD11c, and CD45. Cluster 2 primarily expressed CD8a. Cluster 3 displayed characteristics consistent with mast cells, expressing CD86, CD117, GATA-3, and FoxP3. Cluster 4 was T-bet + memory B-cells, while Clusters 5–8 represented distinct cell populations of NK cells, CD4 + T-cells, neutrophils, and B-cells, as determined by the expression of NK1.1, CD4, Ly6A-E, Siglec-F, MHC-II, and CD19, respectively. Violin graphs illustrate the distribution of cluster sizes across PTD vs TD at the 24-h time point (Fig. 2C). Notably, activated fetal-specific (mT+) macrophages and T-bet + memory B-cells were observed significantly higher incidence in PTD ($p < 0.05$) than TD delivered mice. Moreover, the incidence of CD4 T-cells was higher in TD compared to PTD.

Healthy postpartum mice showed protection from developing HDME-induced lung inflammation

Considering the altered incidence of FMCs across diverse pregnancy conditions, we posited that preterm deliveries could potentially influence the susceptibility of maternal lungs to allergic response and lung

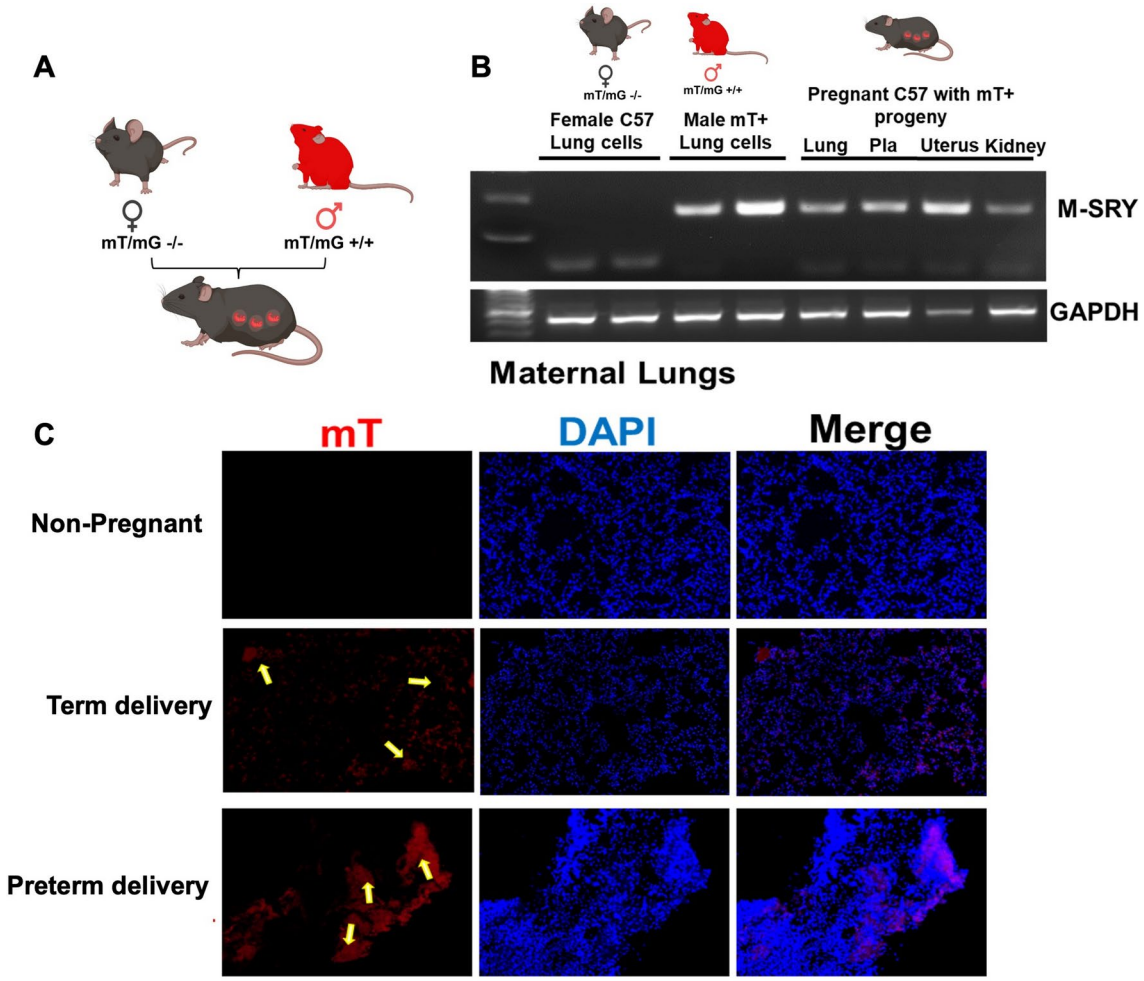

Fig. 1. Characterization of the Cre-reporter transgenic mouse model with membrane-targeted tdTomato (mT). (**A**) Mating strategy to produce mT+—expressing progeny. A two-color fluorescent Cre-reporter allele (mT/mG construct), which has a membrane-targeted tandem dimer Tomato (mT) red fluorescent protein is expressed in all cells and tissues of the progeny. (**B**) PCR revealed the presence of the mouse SRY (M-SRY) gene in the DNA of the cell population extracted from the mT+ cells of different tissues. The positive control DNA was isolated from lung cells of the male TdTomato, and the negative control DNA was isolated from lung cells of the C57 wild-type mice. The PCR product of M-SRY sample was run in the 2% gel. (**C**) Maternal lung tissue sections were imaged under the fluorescence microscope for the presence of mT+ cells (red fluorescence indicated by yellow arrows). We observed an increased in red color intensity (TdTomato) of E. *coli*-treated mice tissues compared to term-delivered mice. This is the representative fluorescence image of the remaining tissues. Flow data represented as the frequency of cell population (mean values) (Fig. 2). Fetal-specific immune cell characterization in maternal lung tissues at different pregnant conditions.

inflammation. To probe the influence of FMCs on maternal lung tissues, we subjected both term and preterm dams to a regimen of PBS and HDME (Fig. 3A). The baseline parameters of Rn were similar between term and preterm mice administered PBS (Fig. 3B). In contrast, the preterm mice challenged with HDME exhibited a 2–4-fold elevation in Rn on average over the other groups at the highest Mch concentrations ($p < 0.05$). They also displayed a concentration-dependent trend across Mch concentrations ranging from 6.25 to 100 mg/mL. Conversely, HDME-exposed healthy, pregnant mice displayed a minimal change in airway hyperresponsiveness, maintaining levels similar to PBS-treated mice.

Notably, HDME-induced allergic asthma is mediated by proinflammatory cytokines such as IL-6, IL-1β, and TGF-α; thus, we assessed the gene expression of these cytokines within the lung tissues. Consistently, the levels of proinflammatory cytokines were markedly elevated in the lungs of HDME-induced mice, regardless of term or preterm pregnancy conditions, in comparison to the PBS controls, as depicted in Fig. 3C. Intriguingly, the mRNA expression of these cytokines demonstrated a significant elevation in the preterm HDME-treated mice as compared to their healthy, full-term delivery counterparts.

Furthermore, HDME treatment prompted considerable airway inflammation in preterm mice as compared to term mice, as evidenced by H&E staining for cellular infiltration, particularly within the peribronchial and perivascular areas of the lung tissues (Fig. 3D). Lastly, consistent with reduced cytokine expression and immune

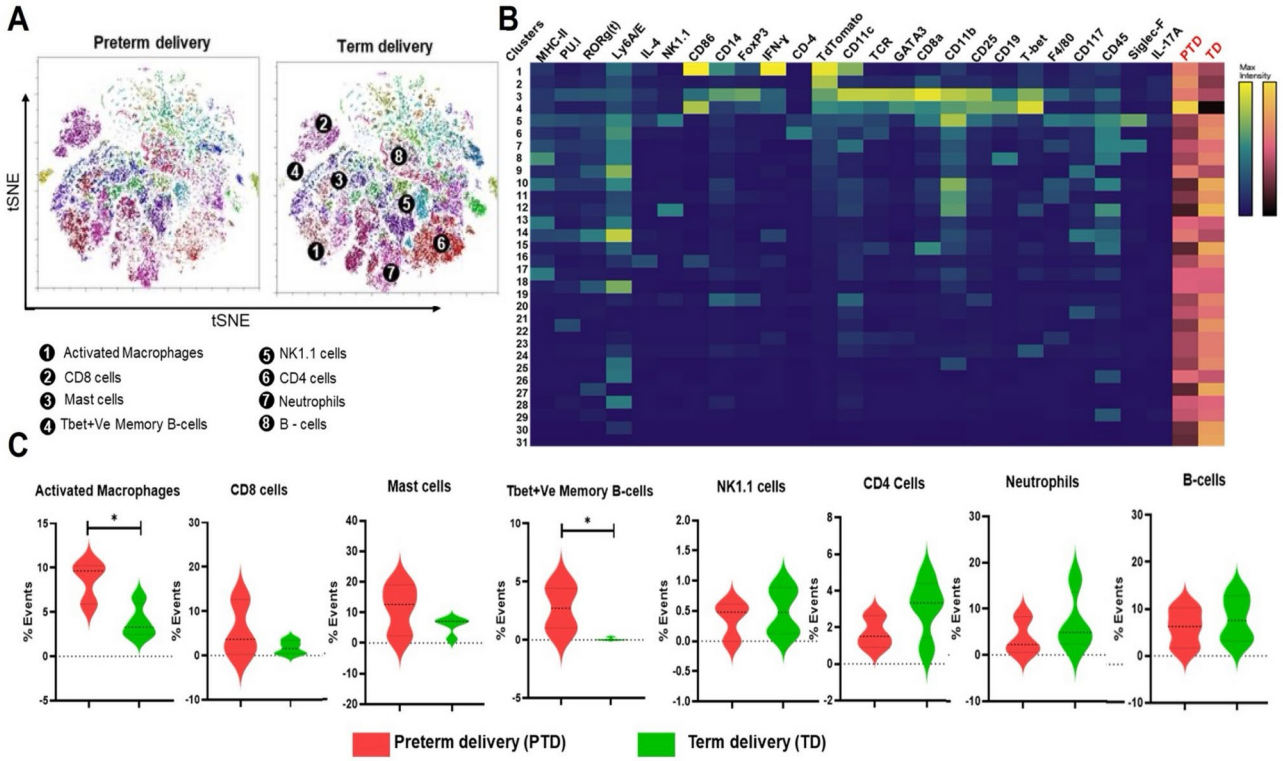

Fig. 2. Fetal-specific immune cell characterization in maternal lung tissues at different pregnant conditions. (**A**) Identification of differentially distributed cellular phenotypes by t-SNE in concatenated PTD vs TD, respectively. (**B**) The heat maps show the relative intensity of each parameter for different clusters in PTD and TD groups. (**C**) The percentage of events of the particular cluster were determined by the bar charts from the cluster explorer tool, and the cluster was characterized by the expression profile expression markers. The characterized clusters percentage events were compared between PTD vs TD. For all groups, $n \geq 5$. Data are shown as mean ± SEM. Data were analyzed using a one-way ANOVA with Tukey's post hoc test. *$p \leq 0.05$, **$p \leq 0.01$, ***$p \leq 0.001$, and ****$p \leq 0.0001$.

cell infiltration, the intensity of PAS-stained goblet cells was qualitatively (visually) higher in preterm-delivered dams after HDME exposure than normal-term deliveries, indicative of the excessive mucus production and airflow obstruction that are hallmarks of allergic asthma (Fig. 3E).

Impact of FMCs from different pregnancy conditions on allergen-induced HSAECs

HSAECs treated with HDME showed a significant increase in the production of proinflammatory cytokines IL-6 and TNF-alpha ($p < 0.01$) (Fig. 4B) compared to those treated with PBS. Surprisingly, in contrast to the above findings, the co-culturing of FMCs derived from term deliveries reduced the cytokine levels (IL-6 sand TNF-alpha) produced by HSAECs treated with HDME. HSAECs co-cultured with preterm FMCs showed significantly ($p < 0.05$) higher levels of pro-inflammatory cytokines than those co-cultured with term FMCs. This finding suggests a potential regulatory role of FMCs from term pregnancies in modulating the inflammatory response triggered by HDME, potentially implicating a mechanism by which these cells exert a dampening effect on the immune response in the context of allergen exposure.

Discussion

To conduct fetal microchimerism assessments prospectively and without bias towards male microchimeric cells, we utilized a Cre-reporter mouse model, which labels fetal cells through fluorescent protein expression, thus permitting functional and mechanistic investigations into this phenomenon[24,30,34]. Our study showed the following: (1) FMCs were found in maternal organs, including the lungs, in both physiologic and pathologic pregnancies, (2) there was a significant increase in the frequency of activated macrophages and Tbet-positive memory B cells in ascending infection-induced PTD than in TD, (3) An exacerbated response to HDME was seen in the lungs of mothers who had ascending infection-associated deliveries, characterized by increased airway resistance, increased pro-inflammatory cytokines, and histologic airway inflammation, and (4) in vitro co-culturing of HSAECs and FMCs corroborated the increase in proinflammatory cytokines in response to HDME in the ascending infection group.

Our murine model reporter showed that the highest frequency of fetal microchimerism ocurred in the maternal lungs[35]. This occurrence is expected, considering the maternal blood circulation from the uterine-draining lymph nodes[36] and broad ligament veins[37] can carry FMCs into the inferior vena cava[37]. Subsequently,

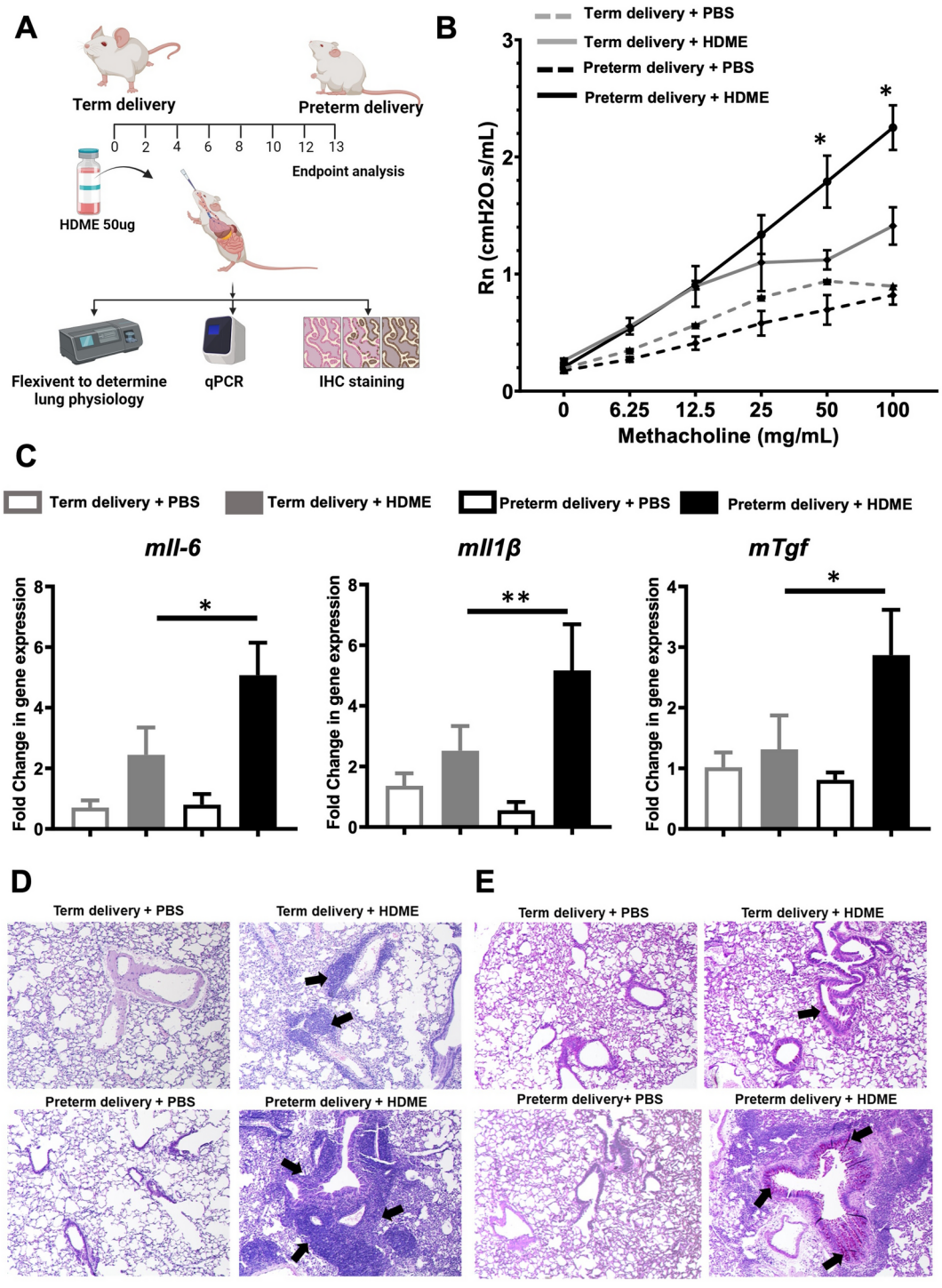

Fig. 3. Effect of pregnancy on developing HDME-induced lung inflammation induced by HDME. (**A**) Experimental design of inducing airway hyperresponsiveness to term and preterm delivery. (**B**) PBS control or HDME-challenged term and preterm delivery were anesthetized 24 h after the HDME challenge and analyzed for AHR. Central airway resistance (R_N) after challenge with increasing doses of MCh was shown ($n = 5$ mice/group; $^*p < 0.05$). (**C**) Lung tissues of the mice were subjected to quantitative real-time PCR for proinflammatory cytokines IL-6, Il-1β, and TGF. Data are presented as mean ± SEM and is pooled from two experiments with a total of three mice for the PBS groups and five mice for the LPS groups. Statistical analysis was performed by two-way ANOVA with the Sidak multiple comparisons test for determining the p values ($^*p < 0.05$; $^{**}p < 0.01$; other comparisons n.s.). (**D**) H&E staining of lung sections of term delivery and preterm-delivered mice administered PBS and HDME intranasally. Scale bar = 100 µm. Representative images of the lungs at 10X magnification are shown. Black arrows indicate cellular infiltration (inflammation) around bronchioles and blood vessels. (**E**) PAS staining of lung sections of term- and preterm-delivered mice administered PBS and HDME intranasally. Scale bar = 100 µm. Representative images of the lungs at 10X magnification are shown. Black arrows indicate PAS positive goblet cells (goblet hyperplasia).

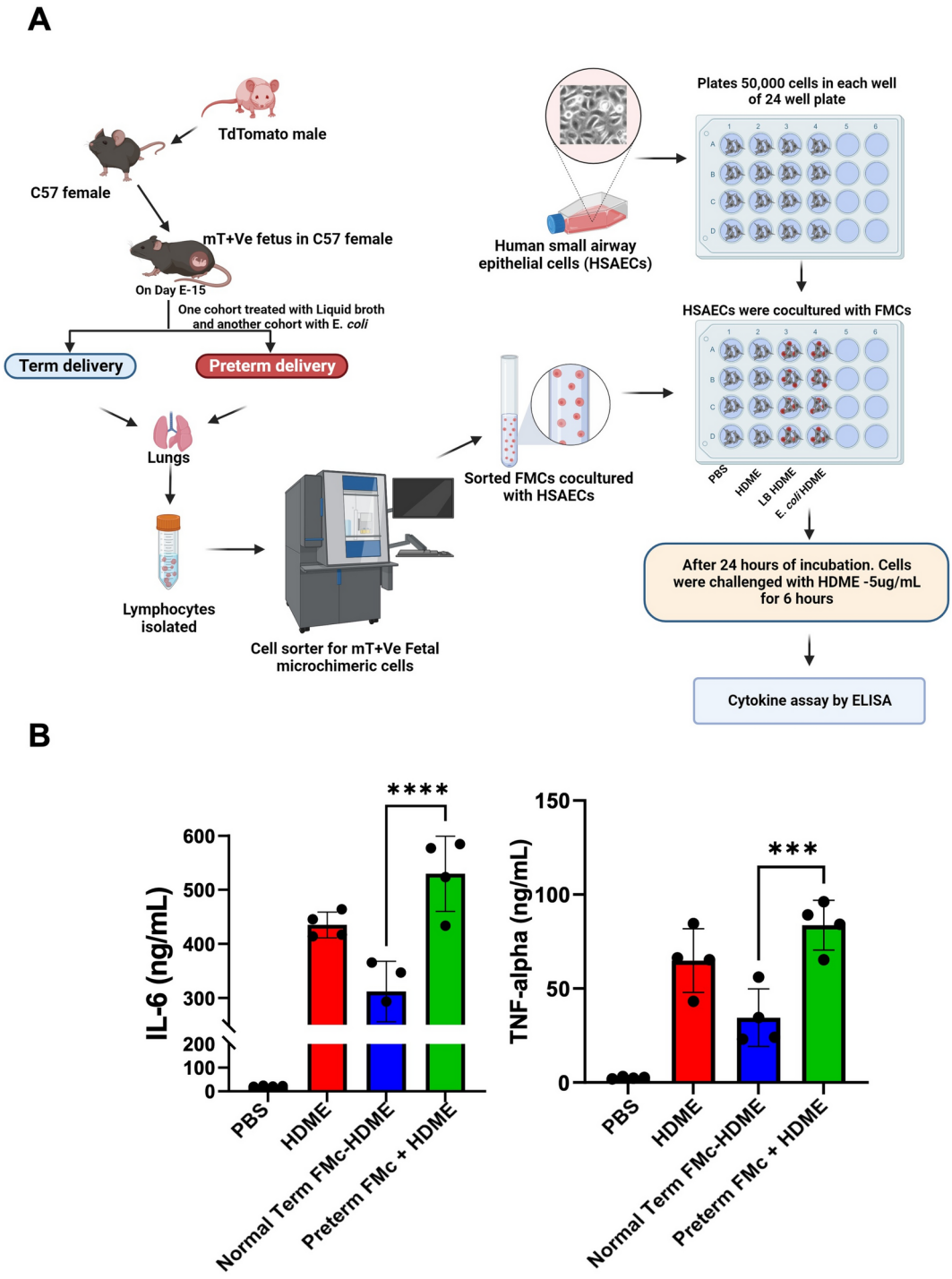

Fig. 4. Functional effect of FMCs in eliciting inflammation in airway epithelial cells. (**A**) Male TdTomato mice were mated with female C57BL/6J mice to generate transgenic mice that express the TdTomato gene in the fetus in the C57 background mice. On day E15, mice were treated with either LB for term delivery or *E. coli* intravaginally to induce preterm delivery. After 48 h, the mice were sacrificed to collect lymphocytes from the lung tissues. Isolated lymphocytes were subjected to flow sorter analysis to sort FMCs in the maternal lungs. FMCs were co-cultured with HSAECs. HSAECs were treated with HDME at a dose of 5ug/mL for 6 h with and without FMCs. After 6 h, the supernatant was collected to perform cytokine analysis by ELISA. (**B**) HSAECs treated with term delivery-derived FMCs showed a decrease in the production of IL-6, whereas the levels increased upon preterm delivery-derived FMCs. Data are represented as mean ± SD. Statistical significance was determined by one-way ANOVA. *$p < 0.05$ and ****$p < 0.0001$.

these cells travel from the right side of the heart to the pulmonary arteries and into pulmonary circulation. However, they undergo rapid clearance at 2.5 weeks postpartum, followed by a gradual decline through at least 90 days postpartum[35]. The pregnancy context influences the persistence of these cells; for instance, in a model of chronic oxidative lung damage due to cigarette smoke exposure during pregnancy, FMCs were retained in maternal lungs longer than in dams without such exposure[38].

A report by Pritchard et al.[8] showed that the three main types of FMCs in maternal lungs were trophoblasts, mesenchymal stem cells, and immune cells. While most trophoblasts are swiftly cleared postpartum in humans, fetal stem cells or immune cells are likely to persist in the maternal lungs[39,40]. Our study confirmed the presence of fetal T cells, NK cells, B cells, mast cells, neutrophils, and macrophages in maternal lungs, irrespective of the pregnancy condition. Further investigation is required to determine whether these cells passively accumulate or participate in the clearance of other FMCs that migrate to maternal lungs.

The higher incidence of microchimeric-activated macrophages in the maternal lungs could significantly impact asthma pathogenesis. While these cells play a protective role against inhaled allergens, depending on the complex set of regulatory networks, they may render maternal lungs more susceptible to inflammation following insult, potentially exacerbating conditions like allergic asthma ([41,42]). Additionally, the increased numbers of T-bet + memory B cells due to PTD could exacerbate inflammatory responses and immune-mediated lung conditions. T-bet + memory B cells are associated with promoting inflammation and immune responses, particularly in allergic reactions and autoimmune diseases. Consequently, an increase in T-bet + memory B cells in the lungs could contribute to conditions such as allergic asthma, characterized by excessive inflammation and immune activity in the airways, leading to symptoms like wheezing, coughing, and difficulty breathing. Moreover, an overactive immune response mediated by T-bet + memory B cells could exacerbate other inflammatory lung conditions, such as chronic obstructive pulmonary disease (COPD) or lung fibrosis[43]. Our study revealed an exacerbated response of PTD dams to HDME, as compared to the physiologic pregnancy group. This was illustrated by an increase in airway resistance, an elevated expression of pro-inflammatory cytokines, leukocyte infiltration, and an increase in goblet cells. Co-culture experiments provided a potential link between the observed pathology and fetal microchimerism, indicating the mechanism by which FMCs can modulate the local tissue microenvironment. Although there are no epidemiologic studies linking preterm delivery to the development of maternal allergic airway disease, evidence suggests that FMCs can modulate disease risk. A study by Thompson et al.[44] showed that maternal microchimerism is a protective factor against the development of asthma in children. However, this study did not provide a mechanistic link regarding how FMCs can predispose maternal lungs to excessive inflammation in the presence of a stressor. Another study by Bustos et al., has demonstrated that patients with hypersensitivity pneumonitis exhibit increased frequency of fetal microchimerism and suggested that microchimeric cells may increase the severity of the disease. Our data, emphasizing the effects on maternal lungs, align with other studies across various organ systems, indicating that pregnancy conditions can modify maternal risk for adverse health outcomes[11,18,45,46].

A major limitation of this study was the utilization of syngeneic mating, which did not fully reflect the semi-allogeneic condition that is pregnancy. This results in the absence of maternal allo-antibodies to paternally derived fetal antigens. Despite this, a maternal immune response can still be induced by Y-chromosome-encoded H-Y antigens[47–49]. Another limitation was the non-characterization of cells other than immune cells. Trophoblasts[8,50], hematopoietic stem cells[51], mesenchymal stem cells[8], and endothelial cells[51] have all been found in maternal lungs, which could play a role in tissue repair and immunomodulation, thus extensive characterization of these other cell types is required in future studies to achieve a more complete picture of the cellular effects.

Despite these limitations, the present study provided new information on the potential postpartum effects of preterm delivery (under conditions of infection-promoting PTD), emphasizing the detrimental impact it can have on maternal lung health. The presence of FMCs, as demonstrated in the research, suggests that preterm pregnancy may predispose the maternal lungs to excessive inflammation when faced with external stressors. This heightened susceptibility could contribute to long-term respiratory issues and could potentially increase the risk of allergic airway disease in affected women; however, the study also highlights a contrasting effect of healthy pregnancy on maternal lung health. It proposes that women who experience uncomplicated pregnancies may benefit from a protective mechanism, which makes them more resilient to the development of long-term respiratory disorders compared to non-pregnant women. This intriguing observation underscores the potential advantages of pregnancy in a woman's lifetime, suggesting that the intricate interplay between fetal microchimerism and maternal immune responses could confer lasting benefits to maternal well-being.

Conclusion

In conclusion, we have provided evidence on how pregnancy conditions can modify maternal risk to adverse health outcomes—in this case, preterm pregnancy and risk of allergic airway disease via fetal microchimerism. This investigation provides an important emphasis on the specific effects within the lung, which can be considered to contribute to the expanding field of fetal microchimerism and its intricate interplay with maternal immune responses. Our findings highlight the intricate interactions between maternal and fetal immune systems, which are influenced by a range of pregnancy conditions. While our study focuses on comparing preterm and term pregnancies, we acknowledge that quantifying the complete dynamic nature of these interactions may require a more-comprehensive analysis, potentially involving a broader panel of cytokines and chemokines. Therefore, we suggest a cautious interpretation of our results in terms of the dynamic nature of maternal–fetal immune interactions under diverse pregnancy conditions. Further research in this field promises to unravel the underlying mechanisms driving these effects, potentially paving the way for strategies to prevent and manage adverse pregnancy-associated maternal morbidities, further emphasizing the importance of maternal–fetal immune interactions in women's health.

Data availability

The datasets generated and/or analyzed during the current study are available from the first and corresponding authors upon reasonable request.

Received: 6 August 2024; Accepted: 11 November 2024
Published online: 18 November 2024

References

1. Sheller-Miller, S. et al. Feto-maternal trafficking of exosomes in murine pregnancy models. *Front. Pharmacol.* **7**, 432 (2016).
2. Kshirsagar, S. K. et al. Immunomodulatory molecules are released from the first trimester and term placenta via exosomes. *Placenta* **33**(12), 982–990 (2012).
3. Yu, J., Ren, X., Cao, S., Li, H. & Hao, X. Beneficial effects of fetal-maternal microchimerism on the activated haplo-identical peripheral blood stem cell treatment for cancer. *Cytotherapy* **10**(4), 331–339 (2008).
4. Gammill, H. S., Aydelotte, T. M., Guthrie, K. A., Nkwopara, E. C. & Nelson, J. L. Cellular fetal microchimerism in preeclampsia. *Hypertension* **62**(6), 1062–1067 (2013).
5. Wang, Y. et al. Fetal cells in mother rats contribute to the remodeling of liver and kidney after injury. *Biochem. Biophys. Res. Commun.* **325**(3), 961–967 (2004).
6. Peterson, S. E., Nelson, J. L., Gadi, V. K. & Gammill, H. S. Fetal cellular microchimerism in miscarriage and pregnancy termination. *Chimerism* **4**(4), 136–138 (2013).
7. Dawe, G. S., Tan, X. W. & Xiao, Z. C. Cell migration from baby to mother. *Cell Adh. Migr.* **1**(1), 19–27 (2007).
8. Pritchard, S., Wick, H. C., Slonim, D. K., Johnson, K. L. & Bianchi, D. W. Comprehensive analysis of genes expressed by rare microchimeric fetal cells in the maternal mouse lung. *Biol. Reprod.* **87**(2), 42 (2012).
9. Bianchi, D. W. Current knowledge about fetal blood cells in the maternal circulation. *J. Perinat. Med.* **26**(3), 175–185 (1998).
10. Adams Waldorf, K. M. et al. Dynamic changes in fetal microchimerism in maternal peripheral blood mononuclear cells, CD4+ and CD8+ cells in normal pregnancy. *Placenta* **31**(7), 589–594 (2010).
11. O'Donoghue, K. Fetal microchimerism and maternal health during and after pregnancy. *Obstet. Med.* **1**(2), 56–64 (2008).
12. Groër, M. W., Manion, M., Szekeres, C. & El-Badri, N. S. Fetal microchimerism and women's health: a new paradigm. *Biol. Res. Nurs.* **13**(4), 346–350 (2011).
13. Broestl, L., Rubin, J. B. & Dahiya, S. Fetal microchimerism in human brain tumors. *Brain Pathol.* **28**(4), 484–494 (2018).
14. Nassar, D., Khosrotehrani, K. & Aractingi, S. Fetal microchimerism in skin wound healing. *Chimerism* **3**(2), 45–47 (2012).
15. Mahmood, U. & O'Donoghue, K. Microchimeric fetal cells play a role in maternal wound healing after pregnancy. *Chimerism* **5**(2), 40–52 (2014).
16. Cirello, V. et al. Fetal cell microchimerism: a protective role in autoimmune thyroid diseases. *Eur. J. Endocrinol.* **173**(1), 111–118 (2015).
17. Fugazzola, L., Cirello, V. & Beck-Peccoz, P. Fetal microchimerism as an explanation of disease. *Nat. Rev. Endocrinol.* **7**(2), 89–97 (2011).
18. Shrivastava, S., Naik, R., Suryawanshi, H. & Gupta, N. Microchimerism: a new concept. *J. Oral Maxillofac. Pathol.* **23**(2), 311 (2019).
19. Gammill, H. S. & Harrington, W. E. Microchimerism: defining and redefining the prepregnancy context—a review. *Placenta* **60**, 130–133 (2017).
20. Vadakke-Madathil, S. & Chaudhry, H. W. Chimerism as the basis for organ repair. *Ann. N. Y. Acad. Sci.* **1487**(1), 12–20 (2021).
21. Lee, E. S., Bou-Gharios, G., Seppanen, E., Khosrotehrani, K. & Fisk, N. M. Fetal stem cell microchimerism: natural-born healers or killers?. *Mol. Hum. Reprod.* **16**(11), 869–878 (2010).
22. Dutta, P. & Burlingham, W. J. Stem cell microchimerism and tolerance to non-inherited maternal antigens. *Chimerism* **1**(1), 2–10 (2010).
23. Adams Waldorf, K. M. & Nelson, J. L. Autoimmune disease during pregnancy and the microchimerism legacy of pregnancy. *Immunol. Invest.* **37**(5), 631–644 (2008).
24. Sheller-Miller, S., Choi, K., Choi, C. & Menon, R. Cyclic-recombinase-reporter mouse model to determine exosome communication and function during pregnancy. *Am. J. Obstet. Gynecol.* **221**(5), 502.e1-.e12 (2019).
25. Sheller-Miller, S., Choi, K., Choi, C. & Menon, R. Cre-reporter mouse model to determine exosome communication and function during pregnancy. *Am. J. Obstet. Gynecol.* (2019).
26. Muzumdar, M. D., Tasic, B., Miyamichi, K., Li, L. & Luo, L. A global double-fluorescent Cre reporter mouse. *Genesis* **45**(9), 593–605 (2007).
27. Percie du Sert, N. et al. The ARRIVE guidelines 2.0: Updated guidelines for reporting animal research. *PLoS Biol.* **18**(7), e3000410 (2020).
28. Spencer, N. R. et al. Development of a mouse model of ascending infection and preterm birth. *PLoS One.* **16**(12), e0260370 (2021).
29. Kammala, A. K. et al. Extracellular vesicles-mediated recombinant IL-10 protects against ascending infection-associated preterm birth by reducing fetal inflammatory response. *Front. Immunol.* **14**, 1196453 (2023).
30. Lintao, R. C. V. et al. Characterization of fetal microchimeric immune cells in mouse maternal hearts during physiologic and pathologic pregnancies. *Front. Cell Dev. Biol.* **2023**, 11 (2023).
31. Hashem, T. et al. CD2 regulates pathogenesis of asthma induced by house dust mice extract. *Front. Immunol.* **11**, 881 (2020).
32. Kammala, A. K. et al. Na+/H+ exchanger regulatory factor 1 mediates the pathogenesis of airway inflammation in a murine model of house dust mite–induced asthma. *J Immunol.* **206**(10), 2301–2311 (2021).
33. Subramanian, H. et al. Ruxolitinib ameliorates airway hyperresponsiveness and lung inflammation in a corticosteroid-resistant murine model of severe asthma. *Front. Immunol.* **12**, 786238 (2021).
34. Sheller-Miller, S. et al. Exosomal delivery of NF-κB inhibitor delays LPS-induced preterm birth and modulates fetal immune cell profile in mouse models. *Sci. Adv.* **7**, 4 (2021).
35. Fujiki, Y., Johnson, K. L., Tighiouart, H., Peter, I. & Bianchi, D. W. Fetomaternal trafficking in the mouse increases as delivery approaches and is highest in the maternal lung. *Biol. Reprod.* **79**(5), 841–848 (2008).
36. Bonney, E. A. & Matzinger, P. The maternal immune system's interaction with circulating fetal cells. *J. Immunol.* **158**(1), 40–47 (1997).
37. Douglas, G. W., Thomas, L., Carr, M., Cullen, N. M. & Morris, R. Trophoblast in the circulating blood during pregnancy. *Am. J. Obstet. Gynecol.* **78**, 960–973 (1959).
38. Vogelgesang, A. et al. Cigarette smoke exposure during pregnancy alters fetomaternal cell trafficking leading to retention of microchimeric cells in the maternal lung. *PLoS One.* **9**(5), e88285 (2014).
39. Attwood, H. D. & Park, W. W. Embolism to the lungs by trophoblast. *J. Obstet. Gynaecol. Br. Commonw.* **68**, 611–617 (1961).
40. Chamley, L. W., Chen, Q., Ding, J., Stone, P. R. & Abumaree, M. Trophoblast deportation: just a waste disposal system or antigen sharing?. *J. Reprod. Immunol.* **88**(2), 99–105 (2011).
41. Fang, S. Y. et al. Distinct phenotypic expression levels of macrophages in neonatal lungs. *Exp. Ther. Med.* **21**(4), 369 (2021).

42. Allard, B., Panariti, A. & Martin, J. G. Alveolar macrophages in the resolution of inflammation, tissue repair, and tolerance to infection. *Front. Immunol.* **9**, 1777 (2018).
43. Finotto, S. et al. Asthmatic changes in mice lacking T-bet are mediated by IL-13. *Int. Immunol.* **17**(8), 993–1007 (2005).
44. Thompson, E. E. et al. Maternal microchimerism protects against the development of asthma. *J. Allergy Clin. Immunol.* **132**(1), 39–44 (2013).
45. Bianchi, D. W. et al. Forever connected: the lifelong biological consequences of fetomaternal and maternofetal microchimerism. *Clin. Chem.* **67**(2), 351–362 (2021).
46. Cómitre-Mariano, B. et al. Feto-maternal microchimerism: memories from pregnancy. *iScience* **25**(1), 103664 (2022).
47. Bonney, E. A. & Onyekwuluje, J. The H-Y response in mid-gestation and long after delivery in mice primed before pregnancy. *Immunol. Invest.* **32**(1–2), 71–81 (2003).
48. Bonney, E. A. & Onyekwuluje, J. Maternal tolerance to H-Y is independent of IL-10. *Immunol. Invest.* **33**(4), 385–395 (2004).
49. Popli, R., Sahaf, B., Nakasone, H., Lee, J. Y. & Miklos, D. B. Clinical impact of H-Y alloimmunity. *Immunol. Res.* **58**(2–3), 249–258 (2014).
50. Schmorl G. *Pathologisch-Anatomische Untersuchungen über Puerperal-Eklampsie* (Vogel, 1893).
51. Fujiki, Y., Johnson, K. L., Peter, I., Tighiouart, H. & Bianchi, D. W. Fetal cells in the pregnant mouse are diverse and express a variety of progenitor and differentiated cell markers. *Biol. Reprod.* **81**(1), 26–32 (2009).
52. Liu, Z., Gu, Y., Shin, A., Zhang, S. & Ginhoux, F. Analysis of myeloid cells in mouse tissues with flow cytometry. *STAR Protoc.* **1**(1), 100029 (2020).
53. Jablonski, K. A. et al. Novel markers to delineate murine M1 and M2 macrophages. *PLoS One* **10**(12), e0145342 (2015).
54. Mily, A et al. Polarization of M1 and M2 human monocyte-derived cells and analysis with flow cytometry upon mycobacterium tuberculosis infection. *J. Vis. Exp.* **2020**, 163 (2020).
55. Harries, M., Hardman, J., Chaudhry, I., Poblet, E. & Paus, R. Profiling the human hair follicle immune system in lichen planopilaris and frontal fibrosing alopecia: can macrophage polarization differentiate these two conditions microscopically?. *Br. J. Dermatol.* **183**(3), 537–547 (2020).
56. Flynn, J. & Gorry, P. Flow cytometry analysis to identify human CD8. *Methods Mol. Biol.* **2048**, 1–13 (2019).
57. Chabot, S. et al. Mouse liver-specific CD8(+) T-cells encounter their cognate antigen and acquire capacity to destroy target hepatocytes. *J. Autoimmun.* **42**, 19–28 (2013).
58. Dahlin, J. S., Ding, Z. & Hallgren, J. Distinguishing mast cell progenitors from mature mast cells in mice. *Stem Cells Dev.* **24**(14), 1703–1711 (2015).
59. Zhou, Y. et al. CD117-positive cells of the heart: progenitor cells or mast cells?. *J. Histochem. Cytochem.* **58**(4), 309–316 (2010).
60. Johnson, B. N. et al. Male microchimerism in females: a quantitative study of twin pedigrees to investigate mechanisms. *Hum. Reprod.* **36**(9), 2529–2537 (2021).
61. Johnson, J. L. et al. The transcription factor T-bet resolves memory B cell subsets with distinct tissue distributions and antibody specificities in mice and humans. *Immunity* **52**(5), 842–55.e6 (2020).
62. Ambegaonkar, A. A., Nagata, S., Pierce, S. K. & Sohn, H. The Differentiation. *Front. Immunol.* **10**, 852 (2019).
63. Dorfman, D. M., Hwang, E. S., Shahsafaei, A. & Glimcher, L. H. T-bet, a T-cell-associated transcription factor, is expressed in a subset of B-cell lymphoproliferative disorders. *Am. J. Clin. Pathol.* **122**(2), 292–297 (2004).
64. Yang, S. Y. et al. A 33-color panel of phenotypic analysis of murine organ specific immune cells. *J. Immunol. Methods* **507**, 113294 (2022).
65. Sahir, F., Mateo, J. M., Steinhoff, M. & Siveen, K. S. Development of a 43 color panel for the characterization of conventional and unconventional T-cell subsets, B cells, NK cells, monocytes, dendritic cells, and innate lymphoid cells using spectral flow cytometry. *Cytometry A* (2020).
66. Oh, J. W., Moon, K. C., Park, C. W., Park, J. S. & Jun, J. K. Acute chorioamnionitis and intra-amniotic inflammation are more severe according to outside-in neutrophil migration within the same chorio-decidua. *Taiwan J. Obstet. Gynecol.* **60**(4), 639–652 (2021).
67. Pfirschke, C. et al. Tumor-Promoting Ly-6G. *Cell Rep.* **32**(12), 108164 (2020).
68. Li, N. et al. Mass cytometry reveals innate lymphoid cell differentiation pathways in the human fetal intestine. *J. Exp. Med.* **215**(5), 1383–1396 (2018).
69. Liechti, T. & Roederer, M. OMIP-060: 30-parameter flow cytometry panel to assess T cell effector functions and regulatory T Cells. *Cytometry A* **95**(11), 1129–1134 (2019).

Acknowledgements

The authors were grateful to Dr.Istvan Boldogh, Professor, Department of Microbiology and Immunology, UTMB for the generous gift of Human small airway epithelial cells (HSAECs). We are thankful to Talar Kechichian for helping us with animal protocol amendments and Phyllis Gamble for her assistance in running the FlexiVent.

Author contributions

A.K. contributed to the conception and design of the research; A.K., R.L., and J.L. contributed to the acquisition and analysis of the data; R.H and J.S. contributed to the interpretation of the data; and A.K, R.L., R.H., B.A., and R.M. contributed to the draft of the manuscript. J.S., B.A., R.M and J.Y. contributed to critical review of the manuscript. All authors agree with the manuscript and declare that the content has not been published elsewhere.

Funding

This study is supported by a seed grant from the endowment funds of Dr. Jerome Yaklic and UTMB IHII Data acquisition grant to Dr. Ananth Kammala and 1R01HD100729 (NIH/NICHD) to Dr. Ramkumar Menon.

Competing interests

The authors state that there are no conflicts of interest regarding this study.

Additional information

Supplementary Information The online version contains supplementary material available at https://doi.org/10.1038/s41598-024-79795-0.

Correspondence and requests for materials should be addressed to A.K.K. or R.M.